# Diffusion of Binary Mixtures in Zeolites: Kinetic Monte Carlo versus Molecular Dynamics Simulations

D. Paschek and R. Krishna*

*Department of Chemical Engineering, University of Amsterdam, Nieuwe Achtergracht 166, 1018 WV Amsterdam, The Netherlands*

*Received May 20, 2000. In Final Form: October 16, 2000*

We report kinetic Monte Carlo (KMC) simulations of self-diffusion of a methane/perfluoromethane mixture in silicalite. The hopping rates and model setup were taken to match previously published MD simulations and PFG-NMR data. In the case of the present KMC simulation the acceleration/deceleration of particles with varying mixture composition can be attributed to correlation effects. The logarithmic interpolation rule for mixture self-diffusion coefficients reported by Snurr and Kärger (*J. Phys. Chem. B* **1997**, *101*, 6469) is validated for a broad range of loadings. However, a deficiency of the present KMC model is that it is not able to cope with different saturation capacities of the two species; the influence of different saturation capacities on mixture diffusion is accounted for by the Maxwell−Stefan theory. The Maxwell−Stefan formulation of diffusion in multicomponent mixtures is used to obtain explicit formulas for calculating the diffusivities of binary mixtures within a zeolite matrix. The theoretical development allows the estimation of the mixture diffusivities on the basis of the pure component diffusivities at zero loadings. We discuss several mixture rules for the estimation of the exchange coefficient $Đ_{12}$. Though none of them is fully satisfying, we demonstrate the $Đ_{12}$ value should have the same order of magnitude as the pure component Maxwell−Stefan diffusivities in order to account properly for acceleration/deceleration behavior.

## Introduction

The proper description of diffusive transport within zeolitic materials is of considerable importance in practice because of the many applications in catalytic reaction and separation processes.[1−3] A variety of models and techniques have been used to describe diffusion within zeolites, ranging from phenomenological models such as the Fick's law of diffusion[1,2] and the Maxwell−Stefan formulation[4,5] to Monte Carlo simulations[6−9] and molecular dynamics (MD).[10,11] In recent years increasing attention has been paid to the description of mixture diffusion[12−15] using MD techniques. The computational expense involved in the use of MD techniques for mixtures is considerable. In this work we study binary mixture diffusion within silicalite using kinetic Monte Carlo (KMC) simulation techniques. The major objective of our work is to examine the extent to which KMC simulation techniques can be used as an alternative to MD techniques to describe mixture diffusion. The KMC approach requires substantially less computational effort than the MD alternative and is therefore appealing. An additional objective of our paper is to highlight an important shortcoming of KMC simulations for mixtures that has not been received due attention in the literature. This shortcoming relates to the inability of the current KMC methodologies to handle mixtures made up of components with different saturation loadings. To compare KMC and MD approaches, we chose the mixture methane/perfluoromethane for study because MD simulation results are already available in the literature.[12]

## Kinetic Monte Carlo Simulations

We perform kinetic Monte Carlo (KMC) simulations of a Langmuir−type system, which means that we have a lattice of equal sites which can be occupied by only one molecule at a time and there are no further molecule−molecule interactions. Particles can move from one site to a neighboring site via hops. The probability per unit time to move from one site to another is determined by transition rates, which have been chosen to reproduce published experimental and simulated (MD-Simulation) data.[12,16]

We employ a standard KMC methodology to propagate the system (see refs 6, 9, 17, and 18). A hop is made every KMC step, and the system clock is updated with variable time steps. For a given configuration of random walkers on the silicalite lattice, a process list containing all possible $M$ moves to vacant sites is created. Each possible move $i$ is associated with a transition probability $k_i$. Note that these values depend on the particular type of move a particle attempts, as well as on the particle type. Now, the *mean* elapsed time $\tau$ is the inverse of the *total* rate coefficient

(1) Kärger, J.; Ruthven, D. M. *Diffusion in Zeolites and Other Microporous Solids*; Wiley & Sons: New York, 1992.
(2) Ruthven, D. M.; Farooq, S.; Knaebel, K. S. *Pressure Swing Adsorption*; VCH Publishers: New York, 1994.
(3) Krishna, R.; Smit, B.; Vlugt, T. J. H. *J. Phys. Chem. A* **1998**, *102*, 7727.
(4) Krishna, R.; Wesselingh, J. A. *Chem. Eng. Sci.* **1997**, *52*, 861.
(5) Kapteijn, F.; Moulijn, J. A.; Krishna, R. *Chem. Eng. Sci.* **2000**, *55*, 2923.
(6) Saravanan, C.; Auerbach, S. M. *J. Chem. Phys.* **1997**, *107*, 8132.
(7) Saravanan, C.; Auerbach, S. M. *J. Chem. Phys.* **1999**, *110*, 11000.
(8) Coppens, M. O.; Bell, A. T.; Chakraborty, A. K. *Chem. Eng. Sci.* **1999**, *54*, 3455.
(9) Paschek, D.; Krishna, R. *Phys. Chem. Chem. Phys.* **2000**, *2*, 2389.
(10) Haberlandt, R.; Fritzsche, S.; Peinel, G.; Heinzinger, K. *Molecular Dynamics*; Vieweg: Braunschweig, 1995.
(11) Pickett, S. D.; Nowak, A. K.; Thomas, J. M.; Peterson, B. K.; Swift, J. F. P.; Cheetham, A. K.; den Ouden, C. J. J.; Smit, B.; Post, M. F. M. *J. Phys. Chem.* **1990**, *94*, 1233.
(12) Snurr, R. Q.; Kärger, J. *J. Phys. Chem. B* **1997**, *101*, 6469.
(13) Jost, S.; Bär, N. K.; Fritzsche, S.; Haberlandt, R.; Kärger, J. *J. Phys. Chem. B* **1998**, *102*, 6375.
(14) Schuring, D.; Jansen, A. P. J.; van Santen, R. A. *J. Phys. Chem. B* **2000**, *104*, 941.
(15) Gergidis, L. N.; Theodorou, D. N. *J. Phys. Chem. B* **1999**, *103*, 3380.
(16) Goodbody, S. J.; Watanabe, K.; MacGowan, D.; Walton, J. P. R. B.; Quirke, N. *J. Chem. Soc., Faraday Trans.* **1991**, *87*, 1951.
(17) Reed, D. A.; Ehrlich, G. *Surf. Sci.* **1981**, *105*, 603.
(18) Fichthorn, K. A.; Weinberg, W. H. *J. Chem. Phys.* **1991**, *95*, 1090.

10.1021/la000695h CCC: $20.00 
Published on Web 12/07/2000

$$\tau^{-1} = k_{\text{total}} = \sum_{i=1}^{M} k_i \tag{1}$$

which is determined as the sum over all processes contained in the process list. The actual KMC time step $\Delta t$ for a given configuration is randomly chosen from a Poisson distribution

$$\Delta t = -\ln(u) k_{\text{total}}^{-1} \tag{2}$$

where $u \in [0,1]$ is a uniform random deviate. The time step $\Delta t$ is independent from the chosen hopping process. To select the actual jump, we define process probabilities according to $p_i = \sum_{j=1}^{i} k_j/k_{\text{total}}$. The $i$th process is chosen, if $p_{i-1} < v \leq p_i$, where $v \in [0,1]$ is another uniform random deviate. After having performed a hop, the process list is updated. To sample ensemble averages correctly and to calculate dynamical properties more easily, the variable time scale is mapped on a periodic time scale for analyzing purposes. [In the KMC simulations presented here the time between two subsequent hopping events follows a Poisson distribution. However, simple dynamic quantities such as the particle mean sqare displacement or time correlation functions in general can be obtained much more easily from a data set, where the time between two stored configurations is constant (as it is done typically in MD simulations). To achieve this, we use a simple bookkeeping procedure, that ensures that a new configuration is only written to the trajectory file, if the system clock has exceeded a certain defined time step value.] To avoid wall effects, we employ periodic boundary conditions. In keeping with our previous findings,[9] the finite size-effect on diffusivity was found to be negligible at a size of $5 \times 5 \times 5$ unit cells. About $10^7$ simulation steps were performed for each simulation. The run length depends strongly on the number of possible jump processes, but even the most time-consuming simulations could be completed within a few hours on a single IBM SP2-node.

To attempt matching the diffusivity data of Goodbody et al.[16] and Snurr and Kärger[12] and to take the correct particle distribution between channel and intersection sites given in ref 12 into account, a discretization of the zeolite channel structure using 24 sites per unit cell is proposed (see Figure 1). Since the present model has been designed to be as simple as possible, the lattice sites are not supposed to represent exactly the minima of the adsorbed particles' potential energy surface but are a coarse grained representation of the channel interior. Moreover, we are neglecting particle-size effects, as well as kinetic correlations in terms of multiple jumps or jump memory (the consequences are discussed in the following sections). The transition probabilities (per unit time) to attempt a hop from a channel site (*st*: straight channel, *zz*: zigzag channel) to any other (neighboring) site are defined by

$$k_{st}(T,\gamma) = k_{st}^{\infty}(\gamma) \exp(-E_a/RT)$$

$$k_{zz}(T,\gamma) = k_{zz}^{\infty}(\gamma) \exp(-E_a/RT) \tag{3}$$

Here, $\gamma$ denotes the particular particle type. $k_{st}^{\infty}(\gamma)$ and $k_{zz}^{\infty}(\gamma)$ define the so-called frequency factors, which characterize individual particle mobilities at infinitely high temperature. For the actual simulations, the rate constants were determined to match the zero-loading self-diffusivities:[12,16] $k_{st}^{\infty}(CH_4) = 2.1 \times 10^{12}$ s$^{-1}$, $k_{st}^{\infty}(CF_4) = 4.5 \times 10^{11}$ s$^{-1}$, $k_{zz}^{\infty}(CH_4) = 1.8 \times 10^{12}$ s$^{-1}$, and $k_{zz}^{\infty}(CF_4) = 3.8 \times 10^{11}$ s$^{-1}$. The temperature dependence is given by assuming Arrhenius behavior of the individual jump rates. The activation energy $E_a$ has been defined to be 4 kJ mol$^{-1}$ in all cases, which is motivated by the temperature dependence of the experimental and MD-Simulation diffusivity data of Snurr and Kärger.[12] To match also the particle distributions given by Snurr and Kärger,[12] the adsorption in channel sites was preferred slightly by reducing the transition probabilities for moves from an intersection site (*in*) to any channel site by a factor of one half

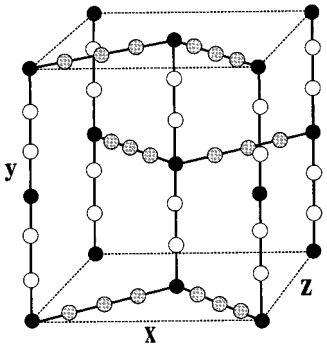


**Figure 1.** Diffusion unit cell used for KMC simulations. Intersection (*in*) sites (black dots) are connected via straight (*st*) channel sites (white dots) and zigzag (*zz*) channel sites (grey dots) (unit cell parameters: $a = 2.01$ nm ($x$), $b = 1.99$ nm ($y$), $c = 1.34$ nm ($z$)).

$$k_{in\rightarrow st}(T,\gamma) = k_{st}(T,\gamma)/2$$

$$k_{in\rightarrow zz}(T,\gamma) = k_{zz}(T,\gamma)/2 \tag{4}$$

A constant factor has been used here, since there is not much information on the temperature dependence of the difference in the sorption strength of channels and intersections. However, large temperature effects are not to be expected, since the difference in sorption strength is rather small, as indicated by the fact that the adsorption data of both components are represented well by a Langmuir single-site isotherm.[19]

Using the setup described above, we obtain a distribution of 1.44 mol/u.c. per intersection site, 4.22 mol/u.c. for the straight channel adsorption, and 6.34 mol/u.c. for the zigzag channel adsorption for both components, methane and perfluoromethane. This is in quite good agreement with the data reported by Snurr and Kärger (see Table 2 in ref 12). To keep the model as simple as possible, we have ignored molecule-size effects. As we will show later, the effect of sizing may lead to problems. In our model, the saturation capacity is naturally fixed to 24 mol/u.c. for both components; therefore, perfluoromethane could be considered as a kinetically slowed version of methane. The implications on mixture diffusion are discussed below.

## Mixture Self-Diffusion

The self-diffusivity tensor may be described by components of the self-diffusion coefficient in the $x$-, $y$- and $z$-directions, which are defined as

$$D_\alpha = \lim_{\Delta t\rightarrow\infty} D_\alpha(\Delta t) = \frac{1}{2} \lim_{\Delta t\rightarrow\infty} \frac{1}{\Delta t} \langle \boldsymbol{r}_\alpha^2(\Delta t) \rangle \tag{5}$$

with $\langle ... \rangle$ denoting both ensemble and time averaging. Accordingly, the average self-diffusion coefficient is ex-

(19) Buss, E.; Heuchel, M. *J. Chem. Soc., Faraday Trans.* **1997**, *93*, 1621.

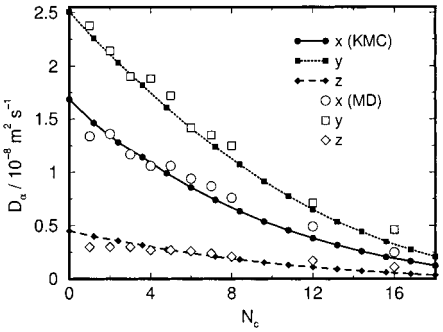


**Figure 2.** Self-diffusion of methane in silicalite in the *x*-, *y*-, and *z*-directions ($T = 300$ K) as a function of the number of adsorbed molecules per unit cell $N_c$. Comparison of KMC simulation results with MD data of Goodbody et al.[16]

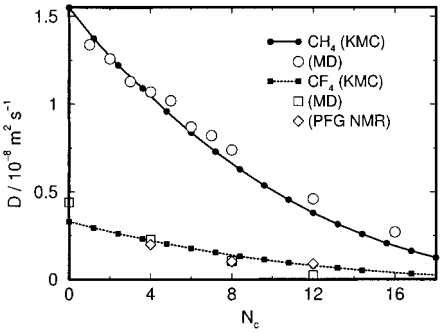


**Figure 3.** Average self-diffusion of methane and perfluoromethane in silicalite ($T = 300$ K) as a function of the number of adsorbed molecules per unit cell $N_c$. Comparison of KMC simulation results with MD data of Goodbody et al.[16] (methane) and MD data and PFG-NMR measurements of Snurr et al.[12] (perfluoromethane).

pressed by

$$D = \frac{1}{3}(D_x + D_y + D_z) \qquad (6)$$

In Figure 2 the components of the self-diffusion coefficients for methane at 300 K obtained from the KMC simulations are compared with the MD simulation data of Goodbody et al.[16] Note the good agreement between the loading dependence of methane for all three directions. So, in addition to the zero-loading diffusivities, which were adjusted in order to match the experimental data, also the model setup seems to be appropriate, since the particular form of the self-diffusivity curve is due to correlation effects,[20] which have been shown to depend strongly on the channel topology.[21] Moreover, since the loading dependence of the pure component self-diffusivities (in all three directions) is described rather well, it does not seem essential to consider additional kinetic correlations in terms of multiple jumps or jump memory effects. While it is possible that such effects may exist, these are apparently of minor importance for the case studied here. It is interesting to note that the deviation from the *mean field* $(1 - \theta)$ behavior found here is even more strongly pronounced than the one obtained recently for 2-methylhexane adsorbed in silicalite.[9] Moreover, we would like to emphasize that the use of a diffusion unit cell that is identical to the crystallographic unit cell gives consistent results with MD simulations. Therefore, the introduction of a particular diffusion unit cell being elongated (doubled) in the *z*-direction, as proposed recently,[22] might be a questionable procedure.

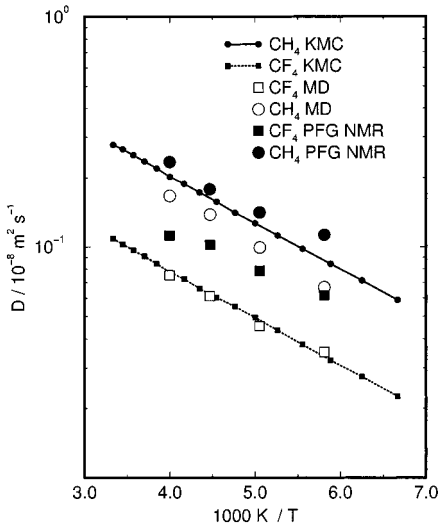


**Figure 4.** Temperature dependence of self-diffusion of methane and perfluoromethane in silicalite at a total loading of eight methane and four perfluoromethane molecules per unit cell. Comparison with data from Snurr and Kärger.[12]

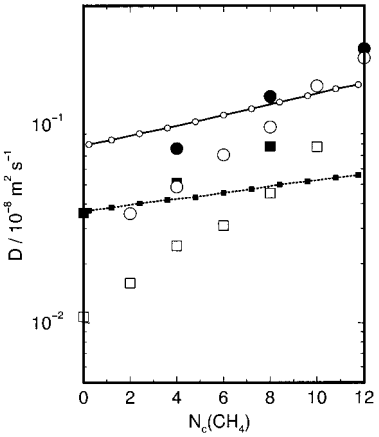


**Figure 5.** Self-diffusion of methane and perfluoromethane in silicalite ($T = 200$ K) at a total loading of $N_c = N_c(CH_4) + N_c(CH_4) = 12$ molecules per unit cell with varying mixture composition. Circles denote methane, and squares indicate perfluoromethane diffusivities. Small symbols denote the KMC simulation results. Large closed symbols denote PFG-NMR, and large open symbols denote MD simulation data according to ref 12.

The average self-diffusion coefficients of pure methane and perfluoromethane at $T = 300$ K are given in Figure 3. Here perfluoromethane is considered to be a kinetically slowed version of methane exhibiting a similar saturation capacity. Considering the large scatter in MD and PFG-NMR data,[12,16] the agreement between KMC simulated data and MD and PFG-NMR data seems to be reasonably good, although the substantially larger value for perfluoromethane at zero loading already indicates that the self-diffusion coefficient of perfluoromethane might decrease somewhat more strongly with loading than that of methane.

The temperature dependence of the self-diffusion coefficients in the mixture at a total loading of eight methane and four perfluoromethane molecules per unit cell is shown in Figure 4. In both cases the KMC data are situated between experimental (PFG-NMR) and MD simulation data. In Figure 5 the self-diffusion coefficients of methane and perfluoromethane are given as a function of composi-

(20) Kärger, J. *J. Phys. Chem.* **1991**, *95*, 5558.
(21) Coppens, M. O.; Bell, A. T.; Chakraborty, A. K. *Chem. Eng. Sci.* **1998**, *53*, 2053.

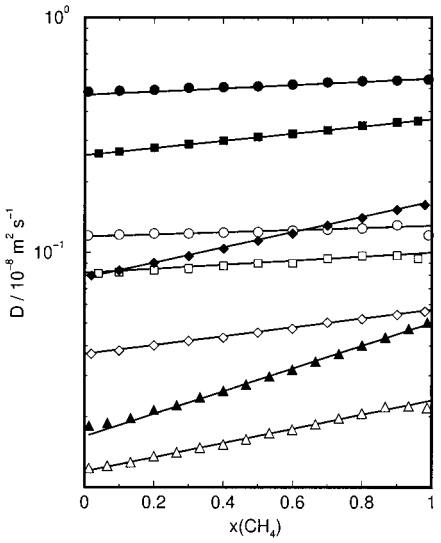


**Figure 6.** Self-diffusion of methane and perfluoromethane in silicalite ($T = 200$ K) at a total loading of 2.4 (circles), 6 (squares), 12 (diamonds), and 18 (triangles) molecules per unit cell as a function of mixture composition. Open symbols indicate the diffusivity of perfluoromethane, while closed symbols represent methane. The straight lines represent fits due to a logarithmic interpolation rule.

**Table 1. Self-diffusion Coefficients of Methane and Perfluoromethane for $x(CH_4) = 0$ and $x(CH_4) = 1$ As a Function of Total Loading**

| | diffusivity in $10^{-8}$ m$^2$ s$^{-1}$ | | | |
|---|---|---|---|---|
| $N_c(CH_4)$ | $D_0(CH_4)$ | $D_1(CH_4)$ | $D_0(CF_4)$ | $D_1(CF_4)$ |
| 2.4 | 0.47 | 0. 55 | 0.117 | 0.130 |
| 6 | 0.26 | 0.37 | 0.082 | 0.010 |
| 12 | 0.078 | 0.165 | 0.037 | 0.057 |
| 18 | 0.0165 | 0.05 | 0.0117 | 0.0235 |

tion at a fixed loading of 12 molecules per unit cell and $T = 200$ K and are compared with the data of Snurr and Kärger. First, we can conclude that KMC simulation, as well as MD simulation and PFG-NMR data, can be described perfectly by a logarithmic interpolation between values for the pure component and at infinite dilution

$$D_1(\Theta,x_1) = D_1(\Theta,x_1=0)^{1-x_1} \times D_1(\Theta,x_1=1)^{x_1}$$

$$D_2(\Theta,x_1) = D_2(\Theta,x_1=0)^{1-x_1} \times D_2(\Theta,x_1=1)^{x_1} \qquad (7)$$

Here, $x_1$ is the molar fraction of species 1 and $D_1(\Theta,x_1)$ and $D_2(\Theta,x_1)$ are the self-diffusion coefficients of species 1 and 2 at a total loading $\Theta = \Theta_1 + \Theta_2$ in molecules per unit cell and composition $x_1$ with

$$x_1 = \frac{\Theta_1}{\Theta_1 + \Theta_2} \qquad (8)$$

Moreover, in Figure 6 it is shown that the apparent validity of the logarithmic interpolation rule can be denoted for the complete range of loadings ranging from 2.4 to 18 molecules per unit cell. With increased loading, the acceleration/deceleration behavior is found to be even more strongly pronounced. The values for $D_{1,2}(\Theta,x_1=0)$ and $D_{1,2}(\Theta,x_1=1)$ obtained from the KMC simulations at 200 K and different total loadings are given in Table 1. However, the slopes of *experimental* (MD simulation and PFG-NMR) and KMC curves in Figure 5 differ notably, so the acceleration/deceleration behavior seems to be underestimated by the KMC model. It is likely that the reason for the weaker composition dependence in the KMC simulations has to be attributed to the effect of different saturation capacities of methane and perfluoromethane. In a previous paper (Paschek and Krishna[9]) we had analyzed in considerable detail the self-diffusivities, the transport diffusivities, and the Maxwell−Stefan diffusivities for single-component diffusion using MC simulations. This study shows clearly that for a system observing the Langmuir isotherm and the absence of any collective dynamics the self-diffusivity tends to zero at saturation loadings; see Figure 6b of ref 9. In the context of self-diffusion in binary mixtures, where the total mixture loading is kept constant, we would expect differences in the sizes of the constituent species and also differences in their saturation loadings to influence component self-diffusivities. Since, for technical reasons, the saturation capacity has to be equal for both components in the KMC model but it is experimentally known that the *slower* component (perfluoromethane) has a significantly smaller saturation limit,[23] it is likely that including the effect of different saturation capacities will increase the diffusivity difference, as reflected in the MD and PFG-NMR data. In a later section we will use Maxwell−Stefan theory in order to support the above-mentioned idea.

## Particle Acceleration/Deceleration: A Correlation Effect

It is interesting to ask why the different particle diffusivities influence each other, since any specific particle−particle interactions are neglected in the Langmuir model. So, the reason for the acceleration/slowing down in the KMC simulations is purely based on the correlation effect. Suppose, a *slow* particle, which is exclusively surrounded by *fast* particles, performs a hop. This initial diffusion step may be canceled (which is the reason for the correlation effect) if the particle performs a hop back. Of course, this can happen only if the vacancy is still in the vicinity of the particle. However, consider the case that the *slow* particle is surrounded by fast particles only. Now it is much more likely for the vacancy to diffuse away compared to a situation where there are only *slow* particles. Therefore, a cancellation of the initial step of the slow particle is less likely, and hence, the diffusive motion of the *slow* particle is, on average, accelerated. The opposite situation is found for the case of a fast particle which is surrounded by *slow* particles. Now, the probability for the *fast* particle to reverse its initial diffusion step is much higher as compared to a situation where also the environment is formed by *fast* particles. Therefore, its correlation factor increases, and hence, the *fast* particle species is slowed. Please note that the acceleration effect is therefore never unique. Since it is based on the correlation effect, its strength will always depend on the lattice topology. Finally, since the correlation effect becomes stronger at higher loadings, the acceleration/deceleration effect also increases.

We would like to point out that the origin of the acceleration/deceleration behavior described here is analogous to what has been recently observed for anisotropic single-component diffusion. For the case of unequal transition probabilities, as for example in the case of diffusion of branched alkanes adsorbed in silicalite, a correlation-effect-based loading dependence of the self-diffusivity tensor could be observed.[9]

(22) Smit, B.; Loyens, L. D. J. C.; Verbist, G. L. M. M. *Faraday Discuss.* **1997**, *106*, 93.
(23) Heuchel, M.; Snurr, R. Q.; Buss, E. *Langmuir* **1997**, *13*, 6795.

### Maxwell−Stefan Theory of Diffusion in Zeolites

The essential concepts behind a general constitutive relation for diffusion in multicomponent mixtures were already available more than a century ago following the pioneering works of James Clerk Maxwell[24] and Josef Stefan.[25] These ideas have been applied to describe diffusion of $n$ species within a zeolite matrix using the following set of equations[4,5]

$$-\rho\frac{\theta_i}{RT}\nabla\mu_i = \sum_{j=1}^{n}(1-\delta_{ij})\frac{\Theta_j\boldsymbol{N}_i - \Theta_i\boldsymbol{N}_j}{\Theta_{i,\mathrm{sat}}\Theta_{j,\mathrm{sat}}Đ_{ij}} + \frac{\boldsymbol{N}_i}{\Theta_{i,\mathrm{sat}}Đ_i}; \quad i = 1, 2, ..., n \tag{9}$$

where $\rho$ is the zeolite matrix density expressed as unit cells per cubic meter, $\Theta_i$ represents the loading expressed in molecules of sorbate per unit cell of zeolite, $\Theta_{i,\mathrm{sat}}$ is the saturation loading of species $i$, $R$ is the gas constant, and $T$ is the temperature. $\nabla\mu_i$ is the gradient of the chemical potential of species $i$, which is the fundamental driving force for diffusion. $\delta_{ij}$ denotes the Kronecker symbol with $\delta_{ij} = 1$ for $i = j$ and $\delta_{ij} = 0$ for $i \neq j$. The fractional occupancy $\theta_i$ of the sorbate within the zeolite matrix is defined as

$$\theta_i \equiv \Theta_i/\Theta_{i,\mathrm{sat}}; \quad i = 1, 2, ..., n \tag{10}$$

In general the saturation loadings of the various species $\Theta_{i,\mathrm{sat}}$ in the mixture will be different from one another. The $\boldsymbol{N}_i$ are the molecular fluxes expressed in terms of molecules transported per square meter per second.

In the Maxwell−Stefan formulation for zeolite diffusion, eq 9, we have to reckon in general with two types of Maxwell−Stefan diffusivities: $Đ_{ij}$ and $Đ_i$. The $Đ_i$ values are the diffusivities which reflect interactions between species $i$ and the zeolite matrix. Mixture diffusion introduces an additional complication due to sorbate−sorbate interactions. The interaction is embodied in the coefficients $Đ_{ij}$. We can consider this coefficient as representing the facility for counter-exchange; that is, at a sorption site the sorbed species $j$ is replaced by the species $i$. The net effect of this counter-exchange is a slowing down of a faster moving species due to interactions with a species of lower mobility. Also, a species of lower mobility is accelerated by interaction with a species of higher mobility.

The Maxwell−Stefan formulation of single-component diffusion can be derived from eq 9 by setting $n = 1$:

$$\boldsymbol{N}_1 = -\rho\Theta_{1,\mathrm{sat}}Đ_1\left(\frac{\theta_1}{RT}\nabla\mu_1\right) \tag{11}$$

where $\mu_1$ is the chemical potential of the sorbed species 1. Assuming equilibrium between the sorbed species and the bulk fluid phase, we have the following relationship for the chemical potential $\mu_1$

$$\mu_1 = \mu_1^\circ + RT\ln(f_1) \tag{12}$$

where $\mu_1^\circ$ is the chemical potential in the chosen standard state and $f_1$ is the fugacity. For not too high system pressures the component partial pressure, $p_1$, can be used in place of the component fugacity, $f_1$; that is, $f_1 \approx p_1$. The chemical potential gradients may be expressed in terms of the gradients of the fractional occupancy, $\nabla\theta_1$

$$\frac{1}{RT}\nabla\mu_1 = \frac{1}{\theta_1}\Gamma\nabla\theta_1; \quad \Gamma \equiv \theta_1\frac{\partial\ln p_1}{\partial\theta_1} \tag{13}$$

where $\Gamma$ is the thermodynamic correction factor. Introducing eq 13 into eq 11, we obtain

$$\boldsymbol{N}_1 = -\rho\Theta_{1,\mathrm{sat}}D_1\nabla\theta_1 = -\rho\Theta_{1,\mathrm{sat}}Đ_1\Gamma\nabla\theta_1 \tag{14}$$

$D_1$ is termed the transport of Fick diffusivity. $Đ_1$ is variously called the Maxwell−Stefan, "corrected" or "jump" diffusivity.[1,4] These two diffusivities are inter-related

$$D_1 = Đ_1\Gamma \tag{15}$$

Often in experiments and simulations, the self-diffusivity of species 1 is determined under conditions where there is no net gradient, $\nabla\theta_1 = 0$. The self-diffusivity shows a decreasing trend with molecular loading; see Figures 2 and 3 for MD simulation results of $CH_4$ and $CF_4$ in silicalite. Monte Carlo simulations have been used recently to show the inter-relationship between self-diffusivities, Maxwell−Stefan diffusivities, and transport diffusivities; see Figure 6b of ref 9. The self-diffusivity is influenced by correlation effects whereas such correlation effects do not affect the Maxwell−Stefan and Fick diffusivities. We note that the Maxwell−Stefan diffusivities follow the simple linear relationship

$$Đ_1 = Đ_1(0)(1-\theta_1) \tag{16}$$

where $Đ_1(0)$ represents the Maxwell−Stefan diffusivity in the limit of zero loading. At zero loading, all three diffusivities, self-diffusivity, Maxwell−Stefan diffusivity, and Fick diffusivity, equal one another. This zero-loading diffusivity can be determined experimentally or by use of transition-state theory.[26]

For a binary mixture, $n = 2$, eq 9 may be cast into two-dimensional matrix notation to give

$$(\boldsymbol{N}) = -\rho[\Theta_{\mathrm{sat}}][B]^{-1}[\Gamma]\nabla(\theta) = -\rho[\Theta_{\mathrm{sat}}][D]\nabla(\theta) \tag{17}$$

where $[D]$ is the two-dimensional Fick diffusivity matrix and $[\Theta_{\mathrm{sat}}]$ is a diagonal matrix with the saturation loadings $\Theta_{i,\mathrm{sat}}$. The matrix $[B]$ has the elements

$$B_{ii} = \frac{1}{Đ_i} + \sum_{j=1}^{n}(1-\delta_{ij})\frac{\theta_j}{Đ_{ij}}; \quad B_{ij} = -\frac{\theta_i}{Đ_{ij}}; \quad i, j = 1, 2, ..., n \tag{18}$$

Taking the inverse of matrix $[B]$ and denoting this as $[S]$, we obtain

$$[B]^{-1} \equiv [S] = \left(1 + \theta_1\frac{Đ_2}{Đ_{12}} + \theta_2\frac{Đ_1}{Đ_{12}}\right)^{-1} \times \begin{bmatrix} Đ_1 + \theta_1\dfrac{Đ_1Đ_2}{Đ_{12}} & \theta_1\dfrac{Đ_1Đ_2}{Đ_{12}} \\ \theta_2\dfrac{Đ_1Đ_2}{Đ_{12}} & Đ_2 + \theta_2\dfrac{Đ_1Đ_2}{Đ_{12}} \end{bmatrix} \tag{19}$$

A procedure for the estimation of the counter-exchange coefficient $Đ_{12}$ has been suggested by Krishna and Wesselingh[4]

(24) Maxwell, J. C. *Philos. Trans. R. Soc.* **1866**, *157*, 49.
(25) Stefan, J. *Sitzber. Akad. Wiss. Wien* **1871**, *63*, 63.
(26) June, R. L.; Bell, A. T.; Theodorou, D. N. *J. Phys. Chem.* **1991**, *95*, 8866.

$$Đ_{12} = Đ_1^{\theta_1/(\theta_1+\theta_2)} Đ_2^{\theta_2/(\theta_1+\theta_2)} \equiv Đ_1^{x_1} Đ_2^{1-x_1} \qquad (20)$$

The matrix [Γ] is the thermodynamic correction factor matrix, which can be determined from the mixture isotherm

$$\Gamma_{ij} \equiv \left(\frac{\Theta_{j,\mathrm{sat}}}{\Theta_{i,\mathrm{sat}}}\right) \frac{\Theta_i}{p_i} \frac{\partial p_i}{\partial \Theta_j}; \quad i, j = 1, 2, ..., n \qquad (21)$$

When the saturation loadings of the two components, $\Theta_{i,\mathrm{sat}}$, are equal to each other and the isotherms of the pure components can be described by a single-site Langmuir isotherm, the matrix of thermodynamic correction factors can be determined from

$$[\Gamma] = \begin{bmatrix} \Gamma_{11} & \Gamma_{12} \\ \Gamma_{21} & \Gamma_{22} \end{bmatrix} = \frac{1}{1-\theta_1-\theta_2} \begin{bmatrix} 1-\theta_2 & \theta_1 \\ \theta_2 & 1-\theta_1 \end{bmatrix} \qquad (22)$$

In the more general case, when the saturation loadings of the two components are different, we have to use the ideal adsorbed solution theory to calculate the mixture isotherms.[5] The recent paper of Kapteijn et al.[5] shows that, for mixtures of light hydrocarbons in silicalite, the IAS theory provides an adequate representation of the sorption isotherm of mixtures in which the constituent species have different sorbate loadings. In more recent papers[27,28] we have shown that for some mixture the real adsorbed solution theory needs to be applied for mixture isotherms.

We could force-fit eq 17 for the two fluxes $\boldsymbol{N}_i$ into the form of Fick's law for each species with effective diffusivities:

$$\boldsymbol{N}_i = -\rho \Theta_{i,\mathrm{sat}} D_{i,\mathrm{eff}} \nabla \theta_i; \quad i = 1, 2 \qquad (23)$$

where the effective Fick diffusivities of components 1 and 2 are given by

$$D_{1,\mathrm{eff}} = D_{11} + D_{12} \frac{\nabla \theta_2}{\nabla \theta_1} \qquad (24)$$

$$D_{2,\mathrm{eff}} = D_{21} \frac{\nabla \theta_1}{\nabla \theta_2} + D_{22} \qquad (25)$$

For self-diffusivity measurements or simulations, the sum of the gradients vanishes; that is

$$\nabla \theta_1 + \nabla \theta_2 = 0 \qquad (26)$$

because the total system loading $(\theta_1 + \theta_2)$ is held constant. In the kinetic Monte Carlo simulations, involving hopping of individual molecules, occupancy gradients of the individual species, $\nabla \theta_i$, are established which have vanishingly small, yet finite, values. For a binary mixture, the gradients of the individual species are equal in magnitude but opposite in sign, satisfying the constraint in eq 26. Invoking this constraint (eq 26), the expression for the self-diffusivities of components 1 and 2 simplifies to

$$\begin{pmatrix} D_{1,\mathrm{eff}} \\ D_{2,\mathrm{eff}} \end{pmatrix} = \begin{pmatrix} D_{11} - D_{12} \\ D_{22} - D_{21} \end{pmatrix} = \begin{pmatrix} S_{11}\Gamma_{11} + S_{12}\Gamma_{21} - S_{11}\Gamma_{12} - S_{12}\Gamma_{22} \\ S_{21}\Gamma_{12} + S_{22}\Gamma_{22} - S_{21}\Gamma_{11} - S_{22}\Gamma_{21} \end{pmatrix} \qquad (27)$$

For the situation in which eq 22 applies, eq 27 further simplifies to

$$\begin{pmatrix} D_{1,\mathrm{eff}} \\ D_{2,\mathrm{eff}} \end{pmatrix} = \begin{pmatrix} S_{11} - S_{12} \\ S_{22} - S_{21} \end{pmatrix} = \left(1 + \theta_1 \frac{Đ_2}{Đ_{12}} + \theta_2 \frac{Đ_1}{Đ_{12}}\right)^{-1} \begin{pmatrix} Đ_1 \\ Đ_2 \end{pmatrix} \qquad (28)$$

Equation 28 represents a remarkably simple result which shows that the self-diffusivities in a binary mixture (supposing the assumptions of eq 22 apply) are not affected by thermodynamic factors and can be determined purely from knowledge of $Đ_1$, $Đ_2$, and $Đ_{12}$. Extending eq 16 to binary mixtures, we take

$$Đ_1 = Đ_1(0)(1 - \theta_1 - \theta_2); \quad Đ_2 = Đ_2(0)(1 - \theta_1 - \theta_2) \qquad (29)$$

and use eq 20 for determination of the counter-exchange coefficient $Đ_{12}$. Equation 29 is a mean field aproach following our earlier paper,[9] extended to mixtures.

We would like to emphasize that the above derivations for the self-diffusivity are different from the model presented by Nelson and Wei,[29] since the Nelson and Wei model ignores the interaction between the species, quantified by the term $Đ_{12}$. Moreover, the Nelson and Wei model does not account for differences in the saturation loadings of the two constituent diffusing species.

## MS Theory versus KMC Simulation

The Maxwell−Stefan formulation takes interaction and correlations between particles into account by using counter-exchange diffusion coefficients $Đ_{ij}$. For a correct description of mixture diffusion, it is therefore essential to be able to reasonably estimate these $Đ_{ij}$ values. Different approaches have been proposed in the literature.[1,4,29,30] Even the most simple one, neglecting the counter-exchange with $Đ_{12} \rightarrow \infty$, has been employed.[1,4,29,30] However, including counter-exchange in terms of the Vignes relation (eq 20) has been shown to work for quite a lot of cases exceptionally well.[4] One advantage of the Maxwell−Stefan formulation is that it gives a thermodynamically consistent description of mixture diffusion and, due to its simplicity, offers the possibility to be used as a tool for the development of technical processes.

Here we are comparing the predictions of MS theory with the proposed KMC model. Since the pure component zero-loading diffusivities ($D_0(CH_4) = 6.95 \times 10^{-9}$ m$^2$ s$^{-1}$ and $D_0(CF_4) = 1.48 \times 10^{-9}$ m$^2$ s$^{-1}$ at $T = 200$ K) as well as the saturation capacities in the KMC model are exactly known, the only fitting parameter left for the description of the mixture diffusion is the choice of the mixture rule for counter-exchange.

In Figures 7 and 8 four different approaches for the estimation of tracer diffusivity are compared with the original KMC self-diffusion data obtained for $T = 200$ K for four different loadings. Ignoring the counter-exchange with $Đ_{12} \rightarrow \infty$, as done in Figure 7a, will lead to complete neglect of the particle acceleration/deceleration behavior. However, giving the counter-exchange coefficient a finite value will account for the acceleration/deceleration, as

(27) Krishna, R.; Paschek, D. *Ind. Eng. Chem. Res.* **2000**, *39*, 2618.
(28) Krishna, R.; Paschek, D. *Sep. Purif. Technol.* **2000**, *21*, 111.
(29) Nelson, P. H.; Wei, J. *J. Catal.* **1992**, *136*, 263.
(30) Wesselingh, J. A.; Krishna, R. *Mass Transfer in Multicomponent Mixtures*; Delft University Press: Delft, 2000.

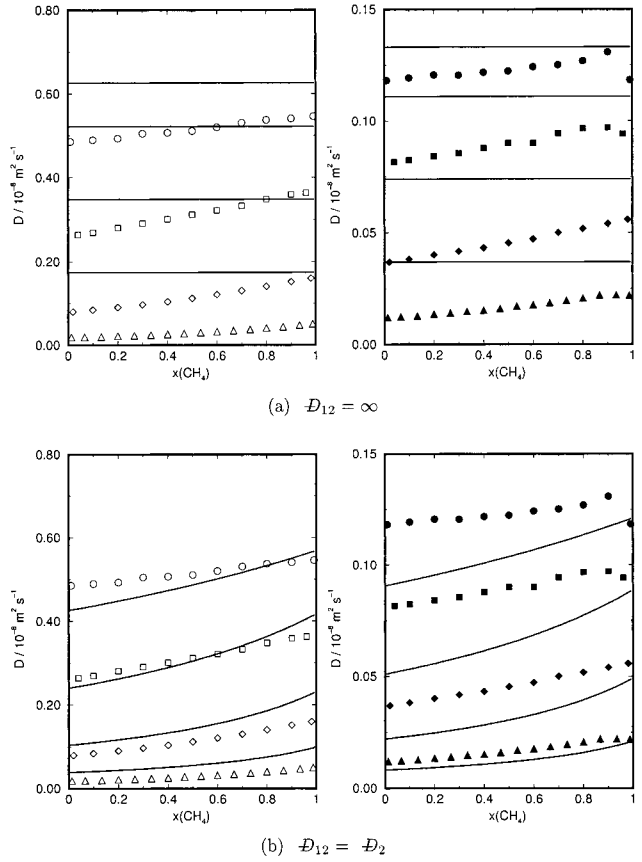


**Figure 7.** Self-diffusion of methane and perfluoromethane in silicalite ($T = 200$ K) at a total loading of 2.4 (circles), 6 (squares), 12 (diamonds), and 18 (triangles) molecules per unit cell as a function of mixture composition. Open symbols indicate the diffusivity of perfluoromethane, while closed symbols represent methane. The straight lines represent predictions due to the Maxwell−Stefan model (eq 28).

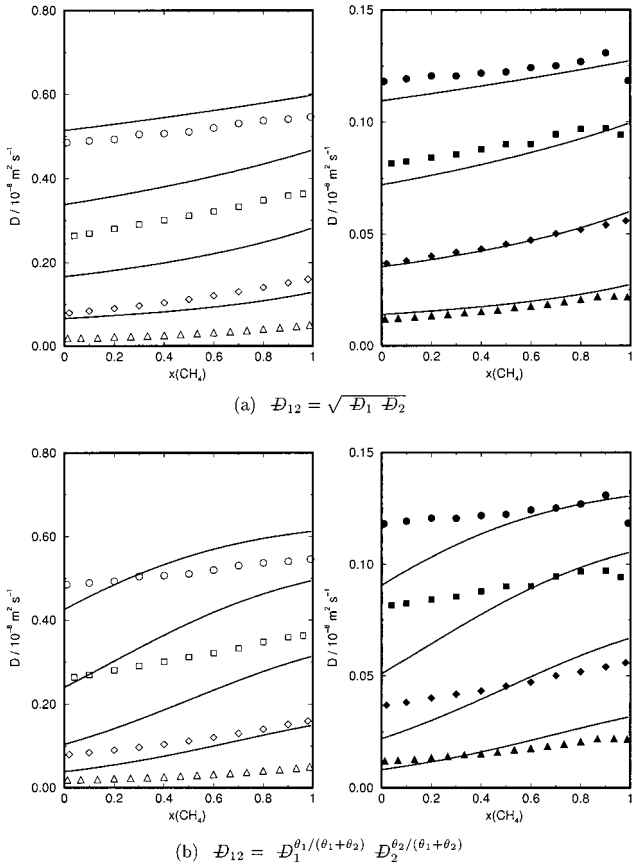


**Figure 8.** Self-diffusion of methane and perfluoromethane in silicalite ($T = 200$ K). The same indication is used as in Figure 7.

can be concluded from Figures 7b and 8a and b. In general, all three approaches employing finite $Đ_{12}$ values are qualitatively more or less correct, since with increasing loading the self-diffusivities tend to become smaller and the acceleration/deceleration effect is present. However, none of them is really satisfying. Taking the value of the slower diffusing species ($Đ_{12} = Đ_2$) gives a good description of the (slower) perfluoromethane diffusivity but a less accurate description of the methane self-diffusion behavior. Using the geometric mean of the diffusivities of the faster and slower components as an estimate ($Đ_{12} = \sqrt{Đ_1 Đ_2}$) will lead to reversed results: In this case the (faster) methane diffusivity is described more accurately than that of perfluoromethane. Finally, the Vignes relation (eq 20) gives *an equally bad* description for both components. This could be an argument in order to use eq 20 instead of others, since no component is favored. We would like to emphasize that none of the mentioned mixture rules are able to account for the apparent logarithmic interpolation behavior deduced from the KMC simulations. So, none of these could be considered as fully satisfying. A more accurate description of the KMC data set would require the exact knowledge of $Đ_{12}$ as a function of loading and composition, rather than the simple approximations provided here. However, since this is a presumably complex function, an exact determination would be only of limited practical interest. Moreover, we would like to stress that this function is not likely to be unique, since the acceleration/deceleration behavior is based on the correlation effect and therefore related to the lattice topology. So we conclude, that in order to account for particle acceleration/deceleration effects, the counter-exchange coefficient should have the same order of magnitude as the pure component Maxwell−Stefan diffusivities.

## Particle-Size Effects

Since the Maxwell−Stefan theory allows us to describe mixture diffusion of particles adsorbed in a microporous material at least on a qualitative level, we would like to demonstrate the influence of different saturation capacities. In Figure 9 the effect is shown for the case of a total loading of 12 molecules per unit cell. Equation 20 was employed as a mixture rule, while the same pure component Maxwell−Stefan zero-loading diffusivities were used as in Figures 7 and 8. A systematic reduction of the saturation capacity of the slower component leads consistently to mixture self-diffusivity curves with increased slope. So, decreasing the saturation capacity for perfluoromethane to 16 molecules per unit cell leads to a far better agreement with the MD-Simulation and PFG-NMR data and underlines the need to account for particle-size effects.

## Conclusions

A simple kinetic model for the mixture diffusion of methane and perfluoromethane adsorbed in silicalite has been proposed. The transition probabilities have been adjusted to match the pure component self-diffusivities at zero loading reported from recent MD simulation and PFG-NMR data. The rather simple KMC model developed here is able to reproduce some basic features basic to methane/perfluoromethane mixture diffusion and tends

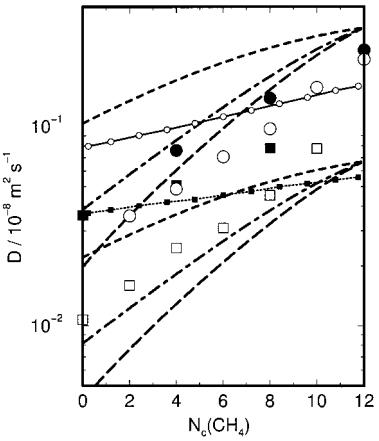


**Figure 9.** Self-diffusion of methane and perfluoromethane in silicalite ($T = 200$ K) at a total loading of $N_c = N_c(CH_4) + N_c(CH_4) = 12$ molecules per unit cell. Indication as in Figure 5. The lines are the Maxwell−Stefan predictions. - - - corresponds to equal saturation capacities (24 mol/u.c.), while - − - corresponds to a reduced saturation capacity of perfluoromethane of 16 mol/u.c. and − − − corresponds to a reduced saturation capacity of perfluoromethane of 14 mol/u.c.

to support the apparent validity of a logarithmic interpolation rule for the mixture self-diffusion coefficients found recently in MD simulations. This is a quite remarkable result, since any particle−particle interactions are absent here and therefore the particle accelerations/decelerations are purely due to correlation effects.

Using the Maxwell−Stefan theory for binary mixture diffusion in zeolites, we have developed explicit formulas, eqs 24 and 25, for calculation of the diffusivities of the components in the mixture. For situations in which the sum of the gradients of the two species is maintained as zero and the assumptions of eq 22 apply, these expressions simplify considerably to yield eq 28, which, when used in conjunction with the explicit mixture rule for estimation of the counter-exchange coefficient $Đ_{12}$, allows the estimation of the mixture diffusivities purely on the basis of the zero-loading diffusivities $Đ_i(0)$. We discuss several mixture rules for the estimation of the exchange coefficient $Đ_{12}$. Though none of them is fully satisfying, we can demonstrate that ignoring the mixture diffusivities ($Đ_{12} \rightarrow \infty$) leads to even worse results. So, we conclude that $Đ_{12}$ should have the same order of magnitude as the pure component Maxwell−Stefan diffusivities in order to account properly for acceleration/deceleration behavior. The Vignes relation (eq 20) turns out to give the best balanced results.

The KMC simulation shown here reveals the importance of accounting for particle-size effects. Since the self-diffusivity of the particles tends to go to zero at maximum loading, different saturation capacities thus influence also the self-diffusion coefficients in the mixture, when equal loadings (molecules per unit cell) are to be considered. In the present KMC model these saturation capacity effects are not included and therefore the mixture behavior is given less accurately than would be possible. However, we have shown that within the framework of Maxwell−Stefan theory these particle-size effects can easily be accounted for.

**Acknowledgment.** The authors acknowledge a grant *Programmasubsidie* from The Netherlands Organization for Scientific Research (NWO) for research on diffusion-selective separation of mixtures. The SCAI Institute at the Gesellschaft für Mathematik and Datenverarbeitung (GMD) in Bonn Sankt Augustin is gratefully acknowledged for providing a generous amount of computer time on their IBM SP2.

LA000695H